

GT2011-45+* %

SIMULATION OF COMBUSTOR DAMAGE MECHANISMS AND MATERIAL SYSTEM PERFORMANCE VIA A SUB-ELEMENT CONFIGURED SPECIMEN TEST

Nagaraja S. Rudrapatna
Honeywell Aerospace
Phoenix, Arizona, USA

Benjamin H. Peterson
Honeywell Aerospace
Phoenix, Arizona, USA

ABSTRACT

Modern gas turbine combustors are made of high temperature alloys, employ effusion cooling and are protected by a Thermal Barrier Coating (TBC). Standard material characterization tests such as creep, oxidation and low cycle fatigue are indicators of a material's potential performance but they neither fully represent the combustor geometric/material system nor fully represent the thermal fatigue conditions a combustor is subjected to during engine operation. Combustor rig tests and/or engine cyclic endurance tests to determine the suitability of new material systems for combustors are time consuming and costly. Therefore, a simple test method for screening material systems under representative combustor conditions is needed.

This experimental system was recently developed at Honeywell Aerospace to characterize various gas turbine combustor damage mechanisms and assess state-of-the-art and developmental materials. A configured specimen is fabricated using materials and processes similarly to actual combustor hardware, including sheet metal forming, welding, TBC coating, and effusion hole laser drilling. The configured specimen is cyclically exposed to hot spot thermal gradients typically experienced by fielded hardware using a jet-fueled burner and heated cooling air. Damage mechanisms simulated include bond coat oxidation, TBC spallation, thermal fatigue and distortion. A summary of these damage mechanisms and lessons learned from test development are presented. Results from recent combustor liner, bond coat, and top coat material modifications are also discussed. The effect of combustor liner material creep and thermal fatigue resistance, bond coat composition and processing, and TBC composition and structure on combustor durability is presented.

INTRODUCTION

Combustor distress is often a result of accumulated damage due to several failure mechanisms such as creep, oxidation and thermal-fatigue. Different failure modes seen in fielded combustor hardware, as shown in Figure 1, include:

- TBC spallation at thermal hot spots and/or at significant temperature gradient locations
- Distorted combustor liners due to substantial plasticity and creep
- Extensive cracking driven by thermal cycling, linking major combustor orifices

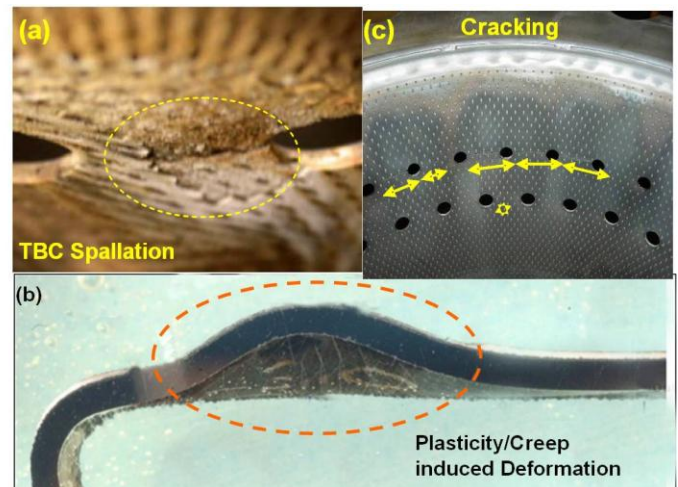


Figure 1: Typical combustor failure modes

In-plane and thru-thickness temperature gradients and thermal cycling are primary contributors to combustor distress. The elevated temperatures associated with the hot spots can cause accelerated bond coat oxidation leading to TBC spallation. Thermal fatigue strains created by local temperature

gradients in combination with geometric/cooling features like effusion holes and/or dilution holes can result in crack formation and propagation in combustor walls. In addition, the resulting distortion at the hot spot disturbs the smooth aerodynamic flow that negatively impacts combustor performance.

Figure 2 shows the cross-section of a typical gas turbine combustor material system. It consists of a metallic substrate, along with a coating system which includes a MCrAlY (M represents a combination of Ni and/or Co) bond coat and a 7 wt% yttria stabilized zirconia (YSZ) thermal barrier coating (TBC). To cover the large surface area of a combustor and to minimize the cost, both bond coat and TBC are generally applied with a plasma spray process in atmosphere (APS). The substrate, a high temperature nickel or cobalt alloy, is typically a sheet metal that can be efficiently fabricated into complex structures for combustor features. The bond coat is an environmental barrier coating for the metallic substrate and a rough surface for the ceramic top-coat to mechanically adhere to. The low-density, porous nature of plasma sprayed TBC reduces heat transfer to the bond coat and substrate due to the relatively low thermal conductivity. The porosity also reduces the modulus of the coating to accommodate strains from the coefficient of thermal expansion (CTE) mismatch with the substrate. Materials with superior properties are continuously sought to improve combustor durability. Improved tensile, fatigue, creep resistance, and environmental resistance (oxidation) of the substrate material should help to prolong the crack initiation and propagation life and reduce distortion that adversely affect combustor aerodynamic performance.

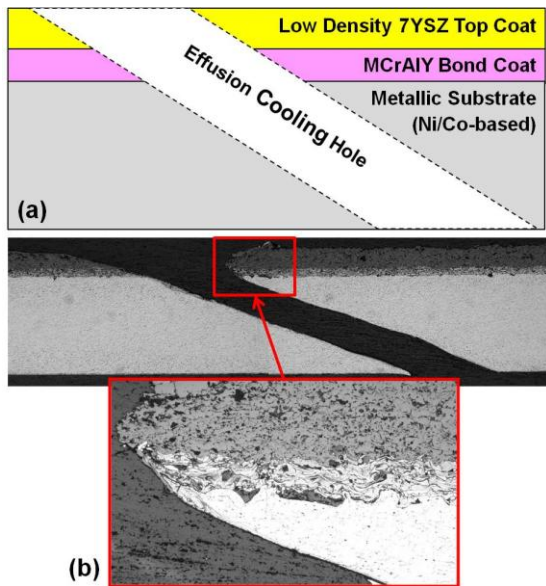


Figure 2: Modern gas turbine combustor material system (a) schematic and (b) optical micrograph of the cross-section

Bond Coat

Two dominant mechanisms that drive TBC failure (spallation) are bond coat oxidation and stresses induced by the gross CTE mismatch between the metallic substrate and the ceramic top-coat. Significant bond coat oxidation as a result of sustained exposure to high temperatures leading to TBC failure is reported in the literature [1-3]. Cappuccini et al. reported results from furnace cycle tests (FCT) on TBC coated buttons that showed heavy oxidation that occurred at a rate of exponential decay. An increase in volume due to oxides results in bi-axial, in-plane compressive stresses during thermo-cycle exposure and failure occurs when the stress exceeds the strength of the oxidized bond coat oxide [4, 5]. Minimizing the formation or presence of oxides in an as-deposited state should increase the useful life of the coating system, thereby increasing combustor life. Low as-deposited oxide content thermal spray options include Low Pressure Plasma Spray (LPPS), argon-shroud plasma spray, and High Velocity Oxygen Fuel (HVOF) spray technique. The first two are modifications of the air plasma spray process, with the general differences being the non-oxidizing atmospheres that they are sprayed in. HVOF employs a high velocity of heated powder to reduce the time between gun and the part surface. All three processes result in a bond coat with low oxide content in the as-deposited state. Isothermal oxidation resistance comparison between air plasma sprayed, vacuum plasma sprayed and HVOF sprayed bond coats is reported by Ferdinando, et al [6].

Thermal Barrier Coating

Exposure to high temperature increases the thermal conductivity due to TBC sintering and closure of the small pores [7]. The presence of alumina and silica in the YSZ TBC negatively impacts the rate of sintering of TBC's [8]. Improved thermal barrier coating composition should improve high temperature performance and enhance combustor durability.

The engine cycle for reduced fuel burn and lower noise requires higher inlet and outlet combustor temperatures. Either cooling flows devoted to provide adequate combustor liner durability will have to increase, or improved material system is needed to meet future demand. Typically, the additional cooling air would come at the expense of emissions and performance, but this will probably not be an option to meet future requirements. Hence, a combination of an improved metallic alloy, for improved crack and distortion resistance, improved bond coat, for reduced oxidation at higher temperatures or longer durations, and a higher temperature capable TBC, for sintering resistance, is required for improving combustor durability and increased temperature performance.

EXPERIMENTAL

A configured specimen test has been recently developed at Honeywell Aerospace to characterize various gas turbine combustor damage mechanisms, assess state-of-the-art, and develop potential future combustor materials and processes [9]. Figure 3 shows a photograph of the test set up. A configured specimen is fabricated with materials and processes similar to actual combustor hardware, including sheet metal forming, welding, TBC coating, and effusion hole laser drilling into a right cylinder that is 4-8” tall and ~8” in diameter. The configured specimen is cyclically exposed to hot spot thermal gradients and temperatures typically experienced by fielded hardware using a jet-fueled burner and heated cooling air. This test is more representative of combustors than coupon-level material evaluation techniques, such as burner bars and furnace cycle tests. The intent of the configured specimen testing is to provide a screening facility to test the durability of candidate materials and coatings, prior to introduction into engine endurance test environments.

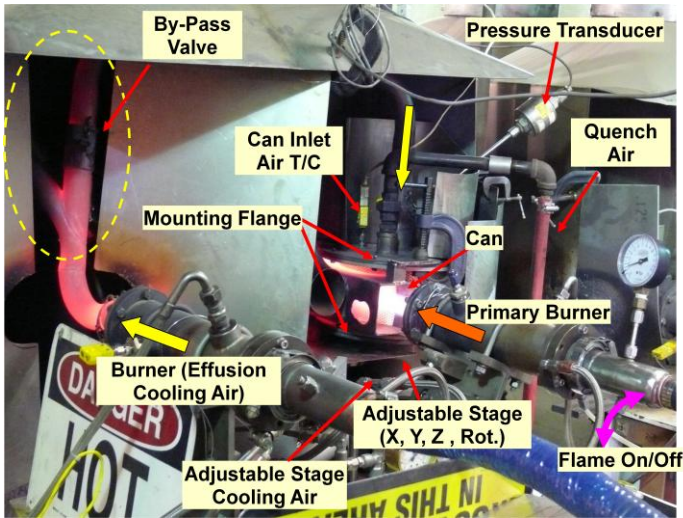


Figure 3: Photograph of the recently developed configured specimen test set-up

Two different high temperature sheet alloys (alloy #1 and alloy #2) are considered for this study. While alloy #1 is a solid solution strengthened nickel-based alloy possessing excellent oxidation resistance and ductility, alloy #2 is an age-hardenable nickel-based super alloy, possessing higher strength, creep/rupture resistance, and fatigue resistance relative to alloy #1.

Table 1 lists the various test specimen configurations discussed in this paper. In addition to the two alloys already mentioned a low oxide content bond coat using the non-APS process and a higher purity TBC were chosen to understand their respective effects on durability, such as: TBC spallation, bond coat oxidation, liner distortion, and liner cracking. Figure

4 shows each of the fabricated configured test specimens, also known as combustor can test specimens. The bond coat thickness, TBC thickness and effusion hole laser drilling parameters were maintained at nominally constant levels to reduce the variation between test specimens.

Table 1: Test specimen details

Test Specimen #	1	2	3	4
Base Material	Alloy #1	Alloy #1	Alloy #1	Alloy #2
Bond Coat	MCrAlY	MCrAlY	MCrAlY	MCrAlY
Method of Spray	APS	APS	Non-APS	APS
Type of TBC	7% YSZ, Std Purity	7% YSZ, High Purity	7% YSZ, High Purity	7% YSZ, Std Purity

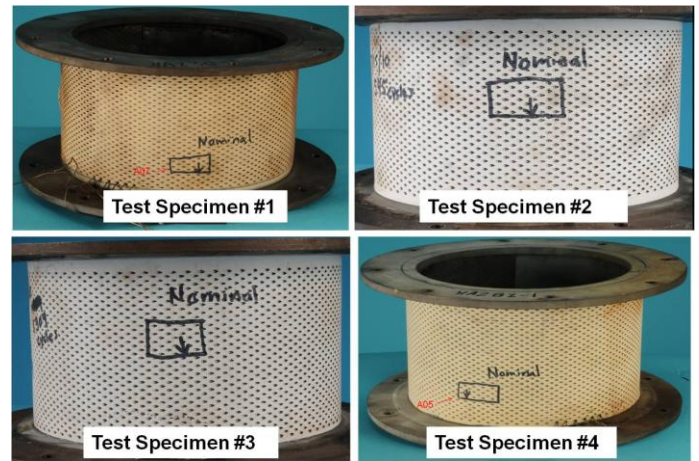


Figure 4: Combustor can test specimens

The specimens were tested at Honeywell’s burner rig facility with a target metal-side peak temperature of 1650°F. The typical thermal cycle profile used to evaluate the performance of the material system is shown in Figure 5a. Figure 5b is a supporting photograph of the corresponding thermocouple locations shown in the plot. Each cycle has a ramp-up event (~2 minutes) to a peak temperature, a soak time (~3 minutes) at peak temperature, followed by a cool down event (~5 minutes). All the combustor can test specimens were subjected to similar thermal wave-forms. The measured test parameters are shown in Table 2 and the test was continued until TBC spallation. Post test visual inspection and metallography were performed to assess the failure mechanisms and damage accumulation in the form of can distortion, bond coat oxidation, and liner cracking.

Table 2: Test parameters

Test Specimen #	1	2	3	4
Peak Temperature (°F)	1647	1659	1659	1656
Temperature Gradient (°F)	93	69	112	138
Minimum Temperature (°F)	195	181	163	178

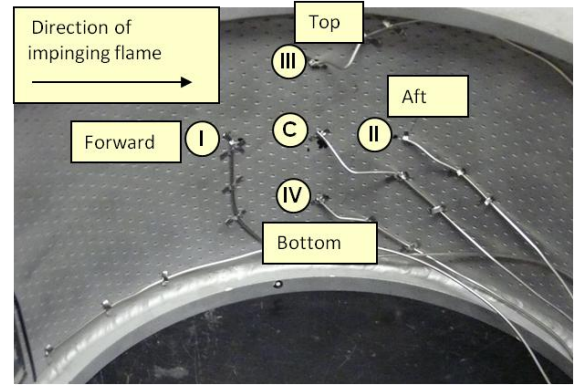
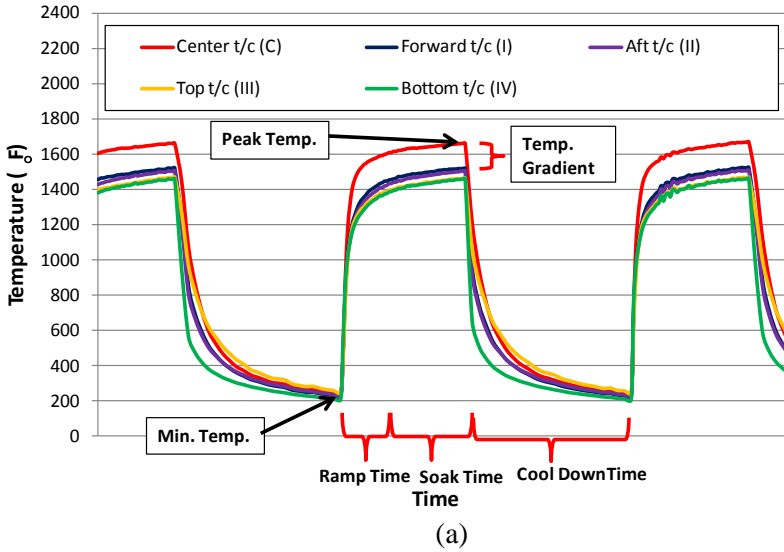


Figure 5: (a) Typical thermal cycle profile and (b) the corresponding thermocouple locations

RESULTS AND DISCUSSION

Figure 6 shows a series of photographs that show an increasingly larger glowing region of TBC between effusion holes over time, which may be indicative of damage evolution. Although not shown, near the time/cycle and location of TBC spallation bright TBC becomes more luminescent in nature, which is characteristic of TBC with an increased surface temperature. This indicates delamination from the substrate/bond coat or bond coat/TBC interface.

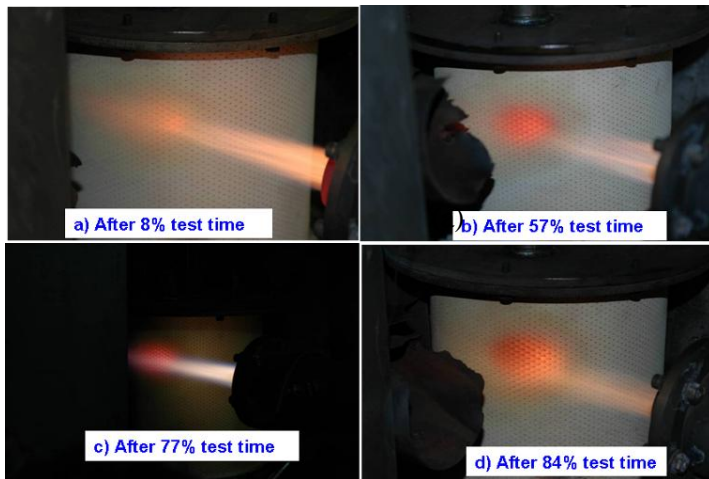


Figure 6: Test specimen failure progression

Figure 7 shows a comparison of the TBC spallation life for each test specimen. The number of cycles to spall TBC is normalized with respect to Specimen #1. The number of cycles to TBC spallation increased two-fold for combustor test

specimens with the non-APS bond coat (Specimen #3) and the alloy #2 material (Specimen #4), as compared with the test specimen with alloy #1 and APS-bond coat (Specimen #1). Figure 8 shows close-up photographs of the TBC spalled regions for all test specimens. For the four specimens reported, the spallation was in the region of the bond coat/TBC interface. Figure 9 is a compilation of optical micrographs of the four test can specimens cross-sectioned near the spalled region and at a nominal location away from the hot spot. The volume fraction of bond coat oxidation values were measured by an area fraction image analysis method. The results imply that a threshold value of about 24-26% bond coat oxidation is achieved at the time of TBC spallation for the APS bond coat. As expected, lower oxide fraction was observed in the non-APS bond coat specimen (Specimen #3).

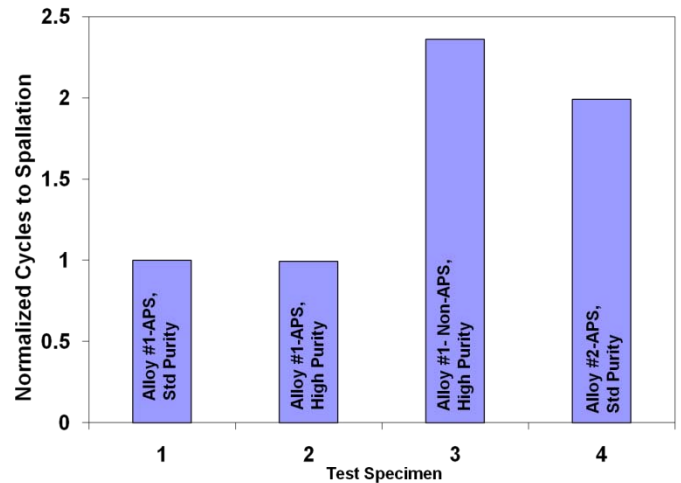


Figure 7: Comparison of the cycles to TBC spallation

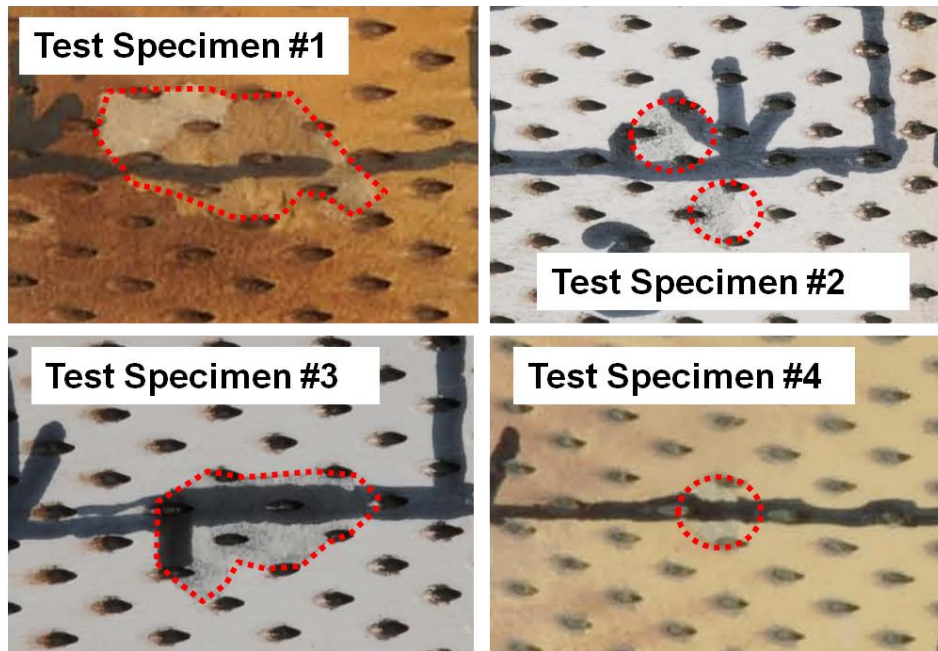


Figure 8: Close-up photographs of the spalled regions (outlined in red).

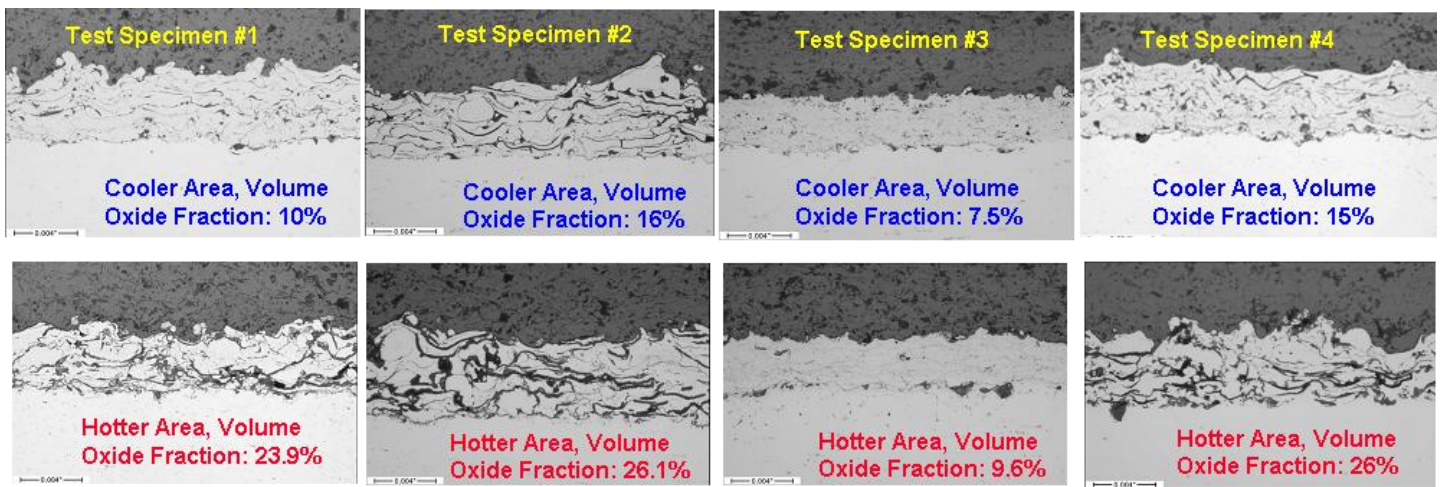


Figure 9: Post-test bond coat oxidation Comparison

TBC spallation is primarily caused by progressive bond coat oxidation and stresses induced by the thermal expansion coefficient (CTE) mismatch between the TBC and bond coat/substrate materials. Lower as-deposited oxide content likely benefited specimen #3. The observed higher life in Specimen #4 is perhaps attributed to higher material strength and creep resistance. Although increased TBC purity (Specimen #2) offers improved sintering resistance, these limited experiments did not demonstrate an increase in spallation life. Higher purity should improve the overall TBC fracture characteristics by maintaining porosity size and distribution as compared with a lower purity 7 wt% YSZ TBC. This should

inhibit the modulus from increasing due to pore closure and maintain the ability to accommodate CTE mismatch strains with the metallic substrate. However, for this test and target temperature, bond coat oxidation may be the dominant mechanism affecting TBC spallation. The TBC is a poor oxygen barrier and correspondingly should not affect the bond coat oxidation rate. The effect of sintering resistance may become more apparent for variations in test conditions, such as higher target temperatures.

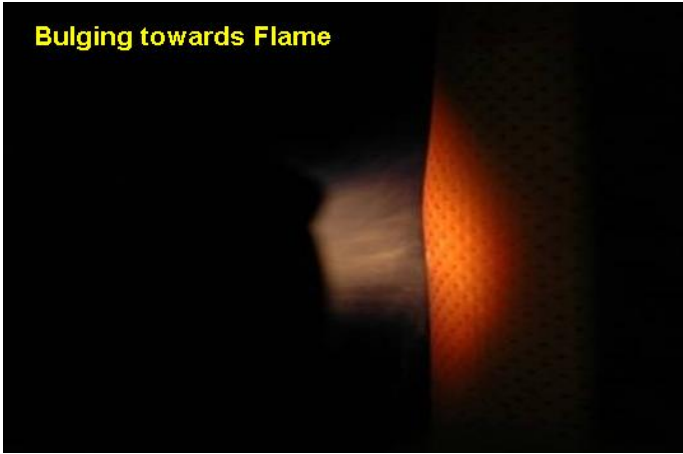


Figure 10: Combustor can deformation during test

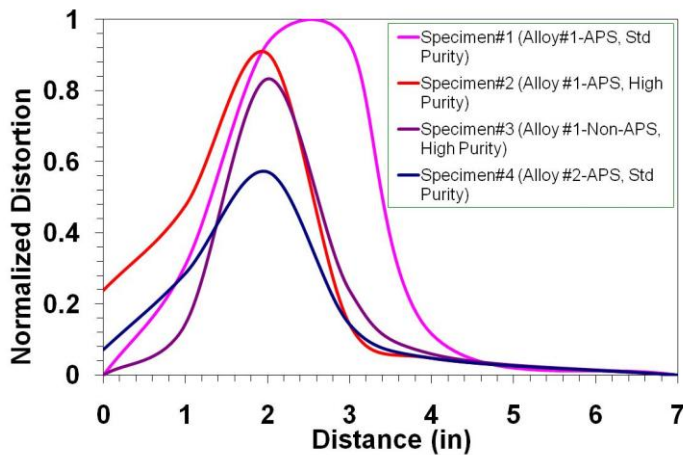


Figure 11: Comparison of permanent deformation

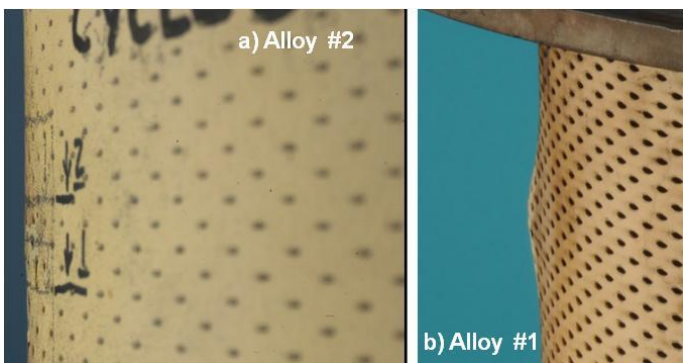


Figure 12: Photographs comparing the post-test combustor can deformation

Figure 10 shows the can deformation towards the flame noticed during the testing of specimen #1. Post test, permanent distortion under the hot spot was measured for each can in line with the direction of the flame (Figure 11). The distortion is driven by the thermal stresses caused by the temperature gradient at the hot spot. The results indicate that the alloy #2 combustor can distortion is about 30-50% lower than the test specimens of alloy #1. Even with a higher temperature gradient (Table 2), the importance of strength and creep resistance is highlighted with a lower magnitude of test can distortion. The similar distortion levels experienced by the cans made of alloy #1 also indicate that the coating system is not a significant influencing parameter. Figure 12 contains the photos of the post-test distortion of the alloy #1 (Specimen #1) and alloy #2 (Specimen #4).

A comparison of measured crack lengths at the edge of effusion holes is shown in Figures 13 and 14. The measured crack length is an indication of the material thermal fatigue performance. The measured crack length for alloy #2 is ~30-50% of cans with alloy #1. This percentage difference in measured crack lengths is similar to the difference in observed permanent distortion. Smaller crack length indicates improved thermal fatigue performance. The smaller crack length in specimen #2 (alloy #1) versus specimen #1 (alloy #1) is attributed to the relatively lower temperature gradient during the test. An even smaller crack length was measured in specimen #3 (alloy #1). Although specimen #3 was subjected to a higher temperature gradient for a longer duration than specimen #2, the crack length variation may be attributed to nominal variations within the laser drilling process.

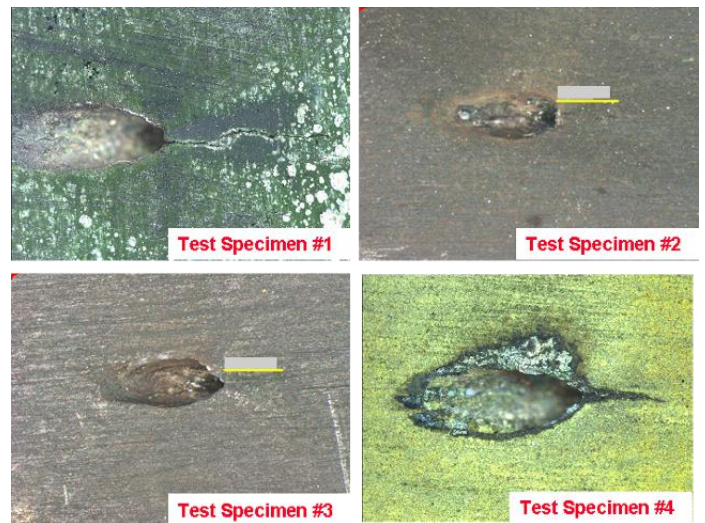


Figure 13: Observed cracks at the edge of effusion hole on the cold side of the combustor can test specimen

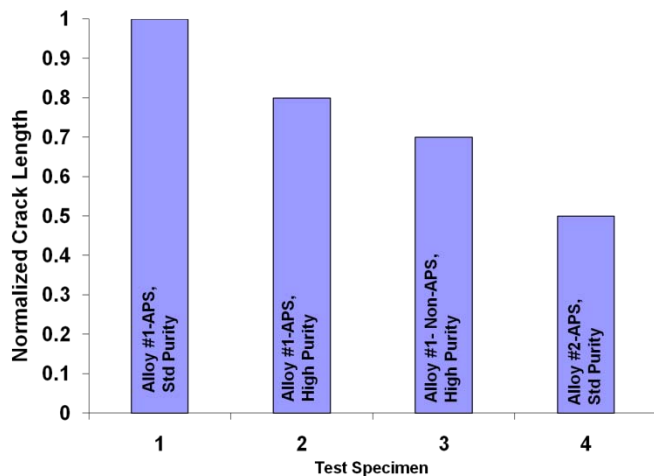


Figure 14: Comparison of measured crack lengths

CONCLUSIONS

Four test specimens were fabricated using the same processes used during actual combustor hardware fabrication including forming, welding, TBC coating, and laser hole drilling. Two high temperature nickel sheet alloys, two bond coats, and two TBC compositional purities were considered. These test specimens were exposed to similar thermal cycles, simulating similar hot spot peak temperatures, which represent thermal hot spots from fielded hardware. Reported data includes cycles to TBC spallation, bond coat oxidation, permanent distortion, and crack length at the edge of effusion holes. Test results based on limited experiments indicate a two fold increase in TBC spallation life for the non-APS bond coat and alloy #2 combustor test specimens, as compared with the alloy #1 test specimens with APS TBC. A significant reduction (~30-50%) in permanent distortion and measured crack lengths at the edge of effusion holes was observed in alloy#2 as compared with alloy#1. Superior spallation life performance of alloy #2 is likely attributed to improved creep resistance. Lower as-deposited oxide content of the non-APS bond coat is attributed to the increased the TBC spallation life observed.

ACKNOWLEDGEMENT

The authors express their thanks to Honeywell for funding. The authors also express their gratitude to James Cobb and Jack McIver at the Honeywell materials testing burner rig lab for their dedicated effort and support during development and testing.

REFERENCES

[1] Cappuccini, F.; Giovannetti, I.; Sanyal, S.; et al, *Damage Evolution & Failure Mechanisms for APS-TBCs*. Proceedings of ASME Turbo Expo 2008, Berlin, Germany, GT2008-50367.

- [2] Chevuru, N.S.; Chan, K.S.; and Gandy, D.W. *Effect of Time and Temperature on Thermal Barrier Coating Failure Mode Under Oxidizing Environment*. Journal of Engineering for Gas Turbines and Power, 2009, **131**/022101-1.
- [3] Chen, W.R.; Wu, X; Marple, B.R.; et al. *Cracking Behaviour of an Air-Plasma Sprayed Thermal Barrier Coating*. Proceedings of ASME Turbo Expo 2009, Orlando, Florida, USA, GT2009-59135.
- [4] Bose, S. and DeMasi-Marcin, J. *Thermal Barrier Coating Experience in Gas Turbine Engines at Pratt & Whitney*. Journal of Thermal Spray Technology, 1997, **6**(1): p. 99-104.
- [5] DeMasi-Marcin, J.T.; Sheffler, K.D.; and Bose, S. *Mechanisms of Degradation and Failure in a Plasma Deposited Thermal Barrier Coating*. Journal of Engineering for Gas Turbines and Power, 1990, **112**/521.
- [6] Di Ferdinando, M.; Fossati, A.; Lavacchi, A.; et al. *Isothermal Oxidation Resistance Comparison between Air Plasma Sprayed, Vacuum Plasma Sprayed and High Velocity Oxygen Fuel Sprayed CoNiCrAlY bond coats*. Surface Coatings and Technology, 2010. **204**: p. 2499-2503.
- [7] Feuerstein, A.; Knapp, J.; Taylor, T.; et al. *Technical and Economical Aspects of Current Thermal Barrier Coating Systems for Gas Turbine Engines by Thermal Spray and EBPVD: A Review*. Journal of Thermal Spray Technology, 2008. **17**(2): p. 199-213.
- [8] Paul, S.; Cipitria, A.; Golosnoy, I.O.; et al. *Effects of Impurity Content on the Sintering Characteristics of Plasma Sprayed Zirconia*. Journal of Thermal Spray Technology, 1997. **16**(5-6): p. 798-802.
- [9] Rudrapatna, N.S.; Peterson, B.H.; and Greving, D. *An Experimental System for Assessing Combustor Durability*. Proceedings of ASME Turbo Expo 2010, Glasgow, UK, GT2010-22150.